

Effect of hydrogen bonding on infrared absorption intensity

Bijjalaxmi Athokpam and Sai G. Ramesh

Department of Inorganic and Physical Chemistry, Indian Institute of Science, Bangalore 560 012, India

Ross H. McKenzie*

School of Mathematics and Physics, University of Queensland, Brisbane 4072, Australia

(Dated: June 15, 2016)

We consider how the infrared intensity of an O-H stretch in a hydrogen bonded complex varies as the strength of the H-bond varies from weak to strong. We obtain trends for the fundamental and overtone transitions as a function of donor-acceptor distance R , which is a common measure of H-bond strength. Our calculations use a simple two-diabatic state model that permits symmetric and asymmetric bonds, i.e. where the proton affinity of the donor and acceptor are equal and unequal, respectively. The dipole moment function uses a Mecke form for the free OH dipole moment, associated with the diabatic states. The transition dipole moment is calculated using one-dimensional vibrational eigenstates associated with the H-atom transfer coordinate on the ground state adiabatic surface of our model. Over 20-fold intensity enhancements for the fundamental are found for strong H-bonds, where there are significant non-Condon effects. The isotope effect on the intensity yields a non-monotonic H/D intensity ratio as a function of R , and is enhanced by the secondary geometric isotope effect. The first overtone intensity is found to vary non-monotonically with H-bond strength; strong enhancements are possible for strong H-bonds. Modifying the dipole moment through the Mecke parameters is found to have a stronger effect on the overtone than the fundamental. We compare our findings with those for specific molecular systems analysed through experiments and theory in earlier works. Our model results compare favourably for strong and medium strength symmetric H-bonds. However, for weak asymmetric bonds we find much smaller effects than in earlier work.

I. INTRODUCTION

A well-known signature of the O-H...O hydrogen (H) bond, in addition to the red-shift of the O-H stretch frequency, is a strong increase in the absorption intensity of the infrared band of this mode.^{1,2} References 3–11 are but a subset of the many works that have previously addressed this effect. The work by Logansen⁷ is particular in that it established an empirical relation between the hydrogen bonding energy and the intensity of the infra-red absorption of the O-H stretching mode for a wide range of compounds:

$$\Delta H = -12.2\Delta(A^{1/2} - A_0^{1/2}), \quad (1)$$

where ΔH is the enthalpy (kJ/mol) of H-bond formation and A and A_0 are the intensities (in units of $10^4 \text{ cm mmol}^{-1} = 100 \text{ km/mol}$) of O-H stretch in the presence and absence of the H-bond respectively. This holds for energies varying by a factor of 200 (between about 0.3 and 60 kJ/mol), thus spanning from weak to strong H-bonds. Ratajczak, Orville-Thomas, and Rao¹² considered a theoretical basis for the empirical relation given in equation (1) using Mullikens charge transfer theory. Rozenberg¹³ recently suggested a relation between H-bond enthalpy and electron density at the bond-critical point from atoms-in-molecules theory, and thereby an indirect linear relation between intensity and electron density. Fillaux⁶, though primarily concerned with the theory of H-bond band shapes, conjectured a non-monotonic relationship between intensity A and the donor-acceptor distance R , with a maximum around $R \simeq 2.6 \text{ \AA}$.

Bratos et al. reviewed experiments describing the variation of the intensity enhancement with the strength of the H-bond⁵. For weak H-bonds ($R > 2.8 \text{ \AA}$) they find enhancement in the range of about 5 to 10. For medium strong H-bonds ($R \sim$

$2.6 - 2.8 \text{ \AA}$), it is enhanced by 10 to 15, while for strong H-bonds it becomes as large as about 30. For strong symmetrical H-bonds ($R < 2.6 \text{ \AA}$), the enhancement of A decreases by about 10 when R decreases from 2.5 to 2.45 \AA , consistent with a non-monotonic dependence on R . However, estimating the intensity accurately is difficult due to the broad spectra.

H/D isotope substitution causes a suppression in the O-H stretch intensity. For free O-H bonds, one anticipates a decrease by a factor of two in the harmonic picture. The suppression changes with H-bond strength as well. For instance, Bratos et al.⁵ state that $A_H/A_D \simeq 2$ for weak H-bonds, which gets enhanced by ~ 2.6 for medium bonds and $\sim 3 - 5$ for strong H-bonds (see note in Ref. 5).

In contrast to the fundamental transition, a number of studies have reported that the intensity of the first overtone of the O-H stretch shows a pronounced suppression upon H-bonding^{9-11,14}. Indeed, eighty years ago failure to observe a OH stretching overtone was correlated with the presence of an H-bond.¹⁵ Di Paolo et al.¹⁴ explained this in terms of a balance between mechanical and electrical anharmonicity. Suhm and co-workers' studies of a range of alcohol dimers^{10,11} report fundamental-to-overtone intensity ratios in the range of 300 to 1000 for the H-bonded OH stretches, compared to about 10 for the monomeric OH. For diols, Howard et al.⁹ found that the suppression increases for the donor O-H with H-bond strength from ethane- (~ 15) to propane- (~ 83) to butanediol (~ 500). The acceptor O-H has a smaller value of about 7. We parenthetically note that the study of overtones is interesting in its own right: Heller¹⁶ pointed out that overtone excitation is a purely quantum effect, associated with dynamical tunneling, just like reflection above a potential barrier. Lehmann and Smith¹⁷ and Medvedev¹⁸ explicitly showed how the transition probability for overtone excitation (i.e. the relevant transition matrix element) is dominated by the semi-classical dynamics

in the classically forbidden region of the potential, particularly the inner wall.

In this paper we study the intensity variation of the O-H stretch transition with H-bond strength using a simple one-dimensional two-state diabatic model potential. Section II discusses the Condon approximation, briefly describes the diabatic model, the computational details, and gives the form of dipole moment function. Section III presents results for the O-H fundamental intensity variation, isotope effect on the fundamental intensity, the first overtone intensity variation, and the effect of modifying the dipole function shape. In Section IV we give a detailed comparison of our results with previous theoretical and experimental works. We offer some remarks in the concluding section.

II. COMPUTATION OF THE INFRARED INTENSITY

The intensity of a vibrational transition $j \leftarrow i$ is experimentally obtained as the integral molar absorption coefficient over the corresponding spectral band,^{7,19}

$$A_{ji} = -\frac{1}{c\ell} \int \ln T(\tilde{\nu}) d\tilde{\nu}. \quad (2)$$

where T is the transmittance, c in the concentration, and ℓ is the path length. The final unit for A_{ji} is km/mol. Time-dependent perturbation theory yields the theoretical expression for the intensity as¹⁹

$$A_{ji} = \frac{2\pi^2}{3\epsilon_0 h c} \tilde{\nu}_{ji} |\mu_{ji}|^2, \quad (3)$$

where the transition dipole matrix element

$$\mu_{ji} = \int dr \phi_j^*(r) \mu_g(r) \phi_i(r) \quad (4)$$

where $\nu_{ji} = E_j - E_i$ and $\phi_i(r)$ is a vibrational wave function and r denotes all the nuclear co-ordinates. For notational simplicity we suppress the vector character of the dipole moment. Here $\tilde{\nu}_{ji}$ is in cm^{-1} , μ is in Debye, and the final units of A_{ji} are again km/mol.

In order to have a sense of the magnitude of A , we note that simple alcohol monomers are reported to have experimental and theoretical gas phase fundamental intensities in the range of about 25 km/mol²⁰⁻²². The corresponding gas phase dimers show an intensity enhancement of about an order of magnitude^{9,10,22}. Experiments by Kuyanov-Prozument et al. on water dimers gives values of 44 and 144 km/mol for the monomer (asymmetric stretch) and dimer, respectively²³.

The *Condon approximation*²⁴ is often applied to Eq. (4). The dipole function enters the intensity expression through its first derivative alone:

$$\mu_{ji} \simeq \mu_{ji}^C \equiv \frac{\partial \mu_g^*(r_{eq})}{\partial r} r_{ji}, \quad (5)$$

where r_{eq} is the equilibrium O-H bond length (i.e. the value of r at which the potential energy is a minimum along the O-H

stretch). Deviations from the Condon approximation are also known as electrical anharmonicity.

The Condon approximation leads to several further analyses. (1) There are two distinct physical mechanisms whereby H-bonding can increase the intensity. The first is by increasing the dipole derivative. The second is by increasing the position matrix element, which will be related to the amount of zero-point motion. (2) If the nuclear wave functions are harmonic, then the only vibrational transition with non-zero intensity is that of the fundamental (i.e. from the ground state $i = 0$ to the first vibrational excited state, $i = 1$). There are no overtones, i.e. higher harmonics. This is known as the *double harmonic approximation*. (The first is the Condon approximation). In reality, all potential energy surfaces are anharmonic and so this leads to the presence of weak overtones in IR spectra. Their intensity can be used to estimate the amount of anharmonicity, both in the potential and the dipole moment surface (i.e. deviations from Condon). In the harmonic approximation, $|r_{01}|^2 \sim \hbar/(m\omega) \propto 1/\sqrt{m}$, where ω is the harmonic frequency of the oscillator. This gives a limiting value for the isotope effect on the fundamental intensity: $A_H/A_D = 2$. (3) The Thomas-Reiche-Kuhn (TRK) sum rule²⁵ relates the oscillator strengths of the ground-to-excited-state transitions:

$$\sum_j (E_j - E_0) |r_{j0}|^2 = \frac{\hbar^2}{2m}. \quad (6)$$

E_j is the energy of the j^{th} vibrational state and m is the reduced mass of the oscillator. This is true for any potential. In the Condon approximation (Eq. (5)), the terms in the summation differ from the intensity (Eq. 3) by a common pre-factor the dipole derivative. Generally, the sum will be dominated by the fundamental. Eq. 6 emphasizes the role of vibrational (mechanical) anharmonicity in the ratio of fundamental-to-overtone intensities.

The intensities of overtones involve contributions from both electrical and mechanical anharmonicities. Early work by di Paolo et al.¹⁴ showed that, for a Morse oscillator with second-order dipole expansions, the two anharmonicities have cancelling influences for the first overtone's intensity while being additive for the fundamental. Ref. 10 found that the relative signs of the dipole moment first and second derivatives for H-bonded OH of 2,2,2-trifluoroethanol dimer to be in agreement with this notion.

Recent works have quantified the effect of the two anharmonicities on the fundamental and overtone intensities of infrared lines for simple molecules. For example, Vazquez and Stanton²⁶ studied H₂O and HFCO, while Banik and Prasad²⁷ studied H₂O and H₂CO. For these simple isolated molecules the effect of the anharmonicities on the intensity of the fundamental is typically only a few per cent.

Whether the assumption of slow variation of the dipole moment over the relevant length scale of the oscillator wave functions is applicable for H-bonded complexes, at various H-bond strengths, is a relevant question. To the extent that it is valid, the other contribution to the intensity is the mechanical anharmonicity. This increases as H-bonding strengthens, which results in an increase in intensity as well. However,

there are significant cases of non-Condon effects. Schmidt, Corcelli, and Skinner²⁸ found that for the OH stretch in liquid water one needs to take into account the dependence of the dipole moment on the nuclear co-ordinates of the surrounding water molecules.

A. Diabatic state model for H-bonding

In this work, we use the two-state diabatic state model for linear symmetric O-H...O H-bonds from recent work by McKenzie²⁹. It was shown in subsequent work^{30,31} that it affords a quantitative description of the correlations observed³² between the OO distance (R) and OH bond lengths (r), the frequencies of OH vibrations (both stretch and bend), and H/D isotope effects for a diverse range of chemical compounds^{30,31}. We use the same notation and parameters as in Ref. 30.

For a O-H...O complex, the Hamiltonian with respect to the diabatic states, $|\text{O-H}\cdots\text{O}\rangle$ and $|\text{O}\cdots\text{H-O}\rangle$, is given as

$$H = \begin{pmatrix} V(r) & \Delta(R) \\ \Delta(R) & V(R-r) + V_o \end{pmatrix} \quad (7)$$

The coordinates r and R are the OH and OO distances, respectively, and r_0 is the equilibrium free OH distance of 0.96 Å. $V(r)$ is Morse potential with a depth (D) of 120 kcal/mol, an exponential parameter (a) of 2.2 \AA^{-1} , corresponding to a harmonic frequency of 3600 cm^{-1} . Its arguments r and $R-r$ in Eq. (10) point to the O-H...O and O...H-O diabats, respectively. V_o is a vertical offset. In this work, we consider both symmetric and asymmetric cases; more details are at the end of this subsection. The coupling between the diabats is given as $\Delta(R) = \Delta_1 \exp(-b(R-R_1))$, with $\Delta_1 = 48 \text{ kcal/mol}$, $b = a$, and $R_1 = 2r_0 + 1/a \approx 2.37 \text{ \AA}$. We note that this is the abbreviated form of the coupling: The full form contains an angular dependence on the two HOO angles as well²⁹.

We treat the donor-acceptor distance R as a control parameter. The electronic ground state for the above Hamiltonian is given as

$$|\Psi_g(r|R)\rangle = -\sin\theta(r|R)|\text{O-H}\cdots\text{O}\rangle + \cos\theta(r|R)|\text{O}\cdots\text{H-O}\rangle \quad (8)$$

where the angle is given by

$$\tan 2\theta(r|R) = \frac{2\Delta(R)}{V(r) - V(R-r) - V_o}. \quad (9)$$

We note that this form for the ground state of the electronic wavefunction allows for the charge transfer character of a H-bond, as emphasized by Thompson and Hynes³³. The potential curve corresponding to this state is

$$\epsilon_-(r, R) = \frac{1}{2} [V(r) + V(R-r) + V_o] - \frac{1}{2} [(V(r) - V(R-r) - V_o)^2 + 4\Delta(R)^2]^{\frac{1}{2}}. \quad (10)$$

For $V_o = 0$, this yields a symmetric double well. This is a suitable choice for strong bonds, since the H atom is essentially shared by the donor and acceptor. In other words, the

respective pK_a 's are about the same³². However, for weak H-bonds, a sizeable V_o is more appropriate. In this work, we consider $V_o = 0$ at all R , and $V_o = 50 \text{ kcal/mol}$ for $R \geq 2.7 \text{ \AA}$. In the latter case, we discuss the variability of the results with asymmetry.

B. Vibrational eigenstates

The vibrational eigenstates used in this work to compute infrared intensities are the 1-D vibrational eigensolutions for a H/D atom on $\epsilon_-(r|R)$. They are calculated using sinc-DVR functions. For the $V_o = 0$ case, the potential is a symmetric double-well. Hence, the solutions are labelled $\phi_{n\pm}$ or n^\pm , where \pm indicates symmetric and antisymmetric tunnel-split doublets. Of course, such a label is truly relevant only if the energy levels are well-below the barrier height. However, we use these labels at all R ; see Ref. 30 for further details. For the asymmetric cases, we simply drop the \pm subscript.

Of primary interest in this work are the ground ($\phi_{0\pm}$ or ϕ_0), first excited ($\phi_{1\pm}$ or ϕ_1), and second excited ($\phi_{2\pm}$ or ϕ_2) states. Transitions between these states define the fundamentals and overtones we analyse.

When H is replaced with D, a secondary geometric isotope effect (SGIE) is observed, wherein the O-O distance changes³⁴⁻³⁶. This is purely a quantum effect based on the vibrational zero-point energy gradients. Within our diabatic model, as the H-bond strengthens from $R = 3.0 \text{ \AA}$ to about $R = 2.45 \text{ \AA}$, deuteration leads to a progressive increase in the O-O equilibrium distance of up to about 0.04 Å. Though small in magnitude, it was found to yield significant H/D frequency effects³⁰. This is because changing R changes the shape of the OH stretch potential, and small changes in R are particularly significant in the regime of low-barrier H-bonds where the energy barrier is comparable to the OH stretch zero point energy. For $R \lesssim 2.4 \text{ \AA}$, the direction of the trend is found to be reversed. In analysing the role of SGIE on the intensities, the eigenenergies and wavefunctions for deuterium are computed at two distances, to wit, without and with the model-estimated O-O distance change. This is carried out only for the symmetric case, $V_o = 0$.

C. Dipole moment for an H-bond, Condon approximation

For the two diabats, the O-H dipole moments point in opposite directions. For a symmetric H-bond, it is then evident that the ground adiabatic state dipole moment function, $\mu_g(r|R)$, would be antisymmetric. To generate such a dipole function, we assume the following form of the *diabatic* dipole function:

$$\hat{\mu}_d = \begin{pmatrix} \mu_0(r) & 0 \\ 0 & -\mu_0(R-r) \end{pmatrix}, \quad (11)$$

where μ_0 is a suitable, common form for the dipole moment of both diabats, and the explicit sign indicates the direction. This is the Mulliken-Hush approach³⁷ where there is no cross term in the diabatic representation of μ . We assume that the choice

of common form of μ_o for both diabats holds for asymmetric potentials as well. This leads to the definition of adiabatic μ_g as

$$\begin{aligned}\mu_g(r|R) &= \langle \Psi_g | \hat{\mu}_d | \Psi_g \rangle \\ &= \sin^2 \theta(r|R) \mu_o(r) - \cos^2 \theta(r|R) \mu_o(R-r) \\ &= \mu_o(r) - \cos^2 \theta(r|R) \{ \mu_o(r) + \mu_o(R-r) \},\end{aligned}\quad (12)$$

where from (9)

$$2 \cos^2 \theta(r|R) = 1 + \frac{V(r) - V(R-r) - V_o}{\sqrt{[V(r) - V(R-r) - V_o]^2 + 4\Delta^2}}.\quad (13)$$

It remains to choose a form for μ_o .

A simple analytical form of a bond dipole moment function is that due to Mecke³⁸:

$$\mu_o(r) = \mu^* r^m \exp(-r/r^*).\quad (14)$$

This has the desired limits that it vanishes for small and large r . We use the Lawton and Child³⁹ parameter values of $m = 1$, $\mu^* = 7.85 \text{ D/\AA}$, and $r^* = 0.6 \text{ \AA}$, originally given for the OH bond in water. The dipole moment has a negative slope at the equilibrium bond length, $r_0 = 0.96 \text{ \AA}$. To a good approximation, for $r \sim 0.8 - 1.8 \text{ \AA}$, which spans the full range of H-bonds, this dipole moment function is linear⁴⁰; compare Figure 5.14 in Ref. 41. Expanding to first order about $r_0 = 0.96 \text{ \AA}$, we get

$$\mu_o(r) = \mu_1 - \mu'(r - r_0).\quad (15)$$

where $\mu_1 = 1.52 \text{ D}$ and $\mu' = 0.95 \text{ D/\AA}$. Note that this linear form corresponds to a Condon approximation for an isolated OH bond. Although all the results we present in the subsequent sections are with the full form of Eq. (14), we note that using the linearized form of μ_o [Eq. (15)] in μ_g yields dipole functions that are slightly different (under about 5%) at various R .

The Condon approximation (Eq. (5)) for $\mu_g(r)$ involves the evaluation of its derivative at $r_{eq}(R)$, which is the minimum of the adiabatic potential $\epsilon_-(r|R)$ at different R . The approximation would be valid to the extent that this shape of μ_g is approximately linear in a sufficiently wide interval about r_{eq} . Below, we will compare the dipole moment function $\mu_g(r)$ with the wavefunction shapes at different R to determine if this is so.

Lastly, we note the selection rules for the fundamental and overtone transitions. Since μ_g is antisymmetric in r for all R , the allowed transitions involve a change in the symmetry of the vibrational wavefunction, i.e., a change in parity. We focus on three transitions: $1^+ \leftarrow 0^-$, $1^- \leftarrow 0^+$, and $2^+ \leftarrow 0^-$. In the next section we discuss the possible identification of these transitions with the fundamental and first overtone. ranges; See also the discussion in Sec. III.V of Ref. 30.

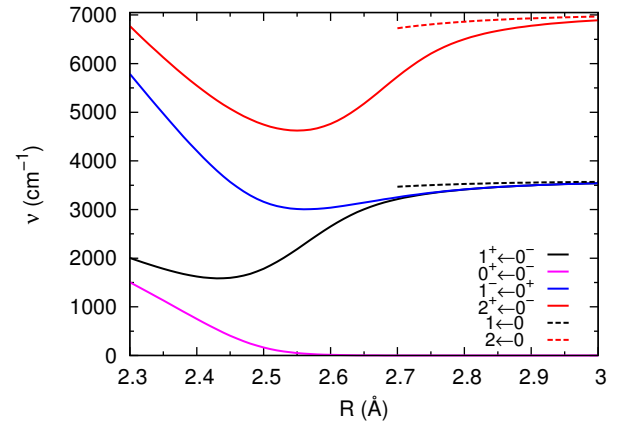


Figure 1: Variation of different OH stretch transition frequencies with the donor acceptor R for symmetric and asymmetric H-bonds. *Solid lines, symmetric H-bonds*: The curves plotted are $1^+ \leftarrow 0^-$ (black), $1^- \leftarrow 0^+$ (blue), $2^+ \leftarrow 0^-$ (red), and $0^+ \leftarrow 0^-$ (magenta). For weak bonds ($R > 2.7 \text{ \AA}$) the black and red curves can be identified with fundamental and first overtone transitions respectively. The blue curve separates from the fundamental curve (solid black) only when the tunnel splitting becomes significant. For moderate bond strengths, the solid black curve has the lowest frequency in the experimentally relevant range ($> 500 \text{ cm}^{-1}$) and so is identified as the fundamental. For strong bonds, there are large anharmonic effects and the nomenclature of fundamental and first overtone is not particularly meaningful. *Dashed lines, asymmetric H-bonds*: The $1 \leftarrow 0$ and $2 \leftarrow 0$ transition frequencies are plotted for $R \geq 2.7 \text{ \AA}$ for an asymmetry (V_o) of 50 kcal/mol. The effective potential of the lower well is a little less anharmonic than for the symmetric case. Consequently, the transition frequencies are a little higher.

III. RESULTS

A. Frequency vs H-bond length (R)

We begin with an analysis of the frequencies of different vibrational transitions as the H-bond strength changes for both symmetric and asymmetric cases. This is necessary, particularly for the symmetric case, to clearly define what we mean by a *fundamental* and a *first overtone*, since there are significant anharmonic effects for strong bonds in the symmetric case. For weak symmetric or weak asymmetric H-bonds, the identification is straightforward.

The solid curves in Figure 1 are for the *symmetric* case. The frequency of the $1^+ \leftarrow 0^-$ transition frequency is seen to have a non-monotonic variation with R (black curve). It is progressively softened (red-shifted) as the H-bond strength changes from weak ($R \gtrsim 2.7 \text{ \AA}$) to moderately strong ($R \sim 2.5 - 2.6 \text{ \AA}$). In the latter region, the barrier height becomes comparable to the energy of the first few O-H vibrational states, and as a result the tunnel-splitting is significant. In the very strong H-bond region ($R < 2.45 \text{ \AA}$), the potential becomes roughly square-well like with a very low or no barrier, and all the vibrational states are energetically well separated. Hence the $1^+ \leftarrow 0^-$ curve turns upward. For moderate bond strengths, the black curve has the lowest frequency in the experimentally

relevant range ($> 500 \text{ cm}^{-1}$) and so is identified as the *fundamental*. The above discussion is based on Figure 3 in Ref. 30 which shows the different potentials and low-lying vibrational energies for $R = 2.3, 2.45, 2.5, 2.9 \text{ \AA}$.

Also shown in Figure 1 (top panel) is the $2^+ \leftarrow 0^-$ transition frequency (red curve). This, too, has a non-monotonic dependence on R . For weak bonds, this can be identified as the *first overtone* as it has roughly twice the frequency of the fundamental. But it turns upward sooner compared to the fundamental since the energy of the 2^+ state, moves higher than the barrier before the 1^+ state does. In the moderate H-bond region, due to significant tunnel-splitting, the $1^- \leftarrow 0^+$ transition frequency (blue curve) clearly separates from the fundamental curve. The definition of the first overtone in this region becomes ambiguous due to the large anharmonicity of the potential. We discuss the intensities for each of these vibrational transitions in Section III D. Like the frequencies, they all have a non-monotonic dependence on R .

We also note that for strong bonds with $R \lesssim 2.5 \text{ \AA}$, the splitting of the 0^+ and 0^- levels becomes larger than 500 cm^{-1} , which is larger than the thermal energy, $k_B T$ at room temperature. This means that the population of the 0^- level will be reduced by a Boltzmann factor of order 0.1. In an experiment, there will be a corresponding reduction in the measured IR absorption intensity associated with transitions from this level. In order to highlight changes in the dipole matrix element, our plots do not take this thermal effect into account.

For the *asymmetric* case, the chosen V_o value shifts the right diabatic in Eq. (7) above the energy of the Morse overtone level of the left (unshifted) diabatic. The resulting ground state potential therefore has *single* and unambiguously identifiable ground, fundamental, and overtone levels. The corresponding wavefunctions are also largely localized on the left side. The fundamental and overtone transition frequencies as a function of R are plotted as red and blue dashed lines in Figure 1. The plots stop at 2.7 \AA since we consider asymmetry only in the weak H-bonding regime. It is of note that the asymmetric fundamental is higher by 256 and 30 cm^{-1} compared to the symmetric case at 2.7 and 3.0 \AA , respectively. The corresponding values for the overtone are 996 and 75 cm^{-1} . Both sets are consistently higher. A major part of these differences is due to the lower harmonic frequency of ground state potential minimum for the $V_o = 0$ case than for $V_o > 0$: The diabatals are more mixed with decreasing asymmetry and at shorter R in general. A smaller role is played by the effective anharmonicity of the ground state potential well, which reduces (to simply the anharmonicity of the Morse potential for the diabatic state) with increasing V_o .

B. Intensity of the fundamental transition and Condon breakdown

For symmetric H-bonds, our calculation of the intensity of the $1^+ \leftarrow 0^-$ (fundamental) transition using eqn. (3) is shown by the solid line in Figure 2. The non-H-bonded OH intensity value (computed at $R = 6.0 \text{ \AA}$) is about 39 km/mol , which compares reasonably with the range of about $20 - 60$

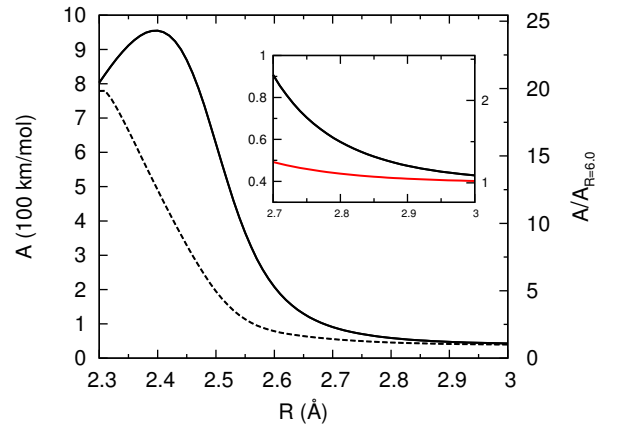


Figure 2: Intensity of the $1^+ \leftarrow 0^-$ transition as a function of R . The left axis is intensity in (100 km/mol) units and the right axis is the intensity scaled with respect to its value for $R = 6.0 \text{ \AA}$ (non-H-bonded OH). The solid line is the intensity obtained through the full matrix element, Eqn.(4), while the dashed line is obtained using the Condon approximation, eqn. (5). The inset is a blow-up of the curve, showing the relatively small intensity enhancements in the weak H-bond regime. Also shown in red in the inset is the trend when $V_o = 50 \text{ kcal/mol}$.

km/mol reported for O-H stretches for a range of isolated molecules^{20–22,27}. The intensity enhancement relative to this value is a little over 2 in the weak H-bond region (see inset). As the curve enters the moderately strong H-bond region ($R \lesssim 2.6 \text{ \AA}$), it shows $\sim 5 - 10$ fold enhancement, reaching ~ 20 for strong H-bonds ($R \approx 2.4 \text{ \AA}$). Broadly, this agrees with experimental results summarised by Bratos et al.⁵.

Figure 3 shows the contributions to the integrand in eqn. (4), viz. $\mu_g(r)$ and $\phi_{1^+}\phi_{0^-}(r)$, at different R , giving insight into the intensity enhancement with increased H-bond strength. These functions are both asymmetric about $r - R/2 = 0$ at all R . Hence it would suffice to consider only one vertical half of the plots. The top panel is for $R = 2.8 \text{ \AA}$. Here, $\mu_g(r)$ is mostly linear for a large O-H distance (r) range. The $\phi_{1^+}\phi_{0^-}$ product function amplitude is non-zero over roughly the same r range. Its positive and negative regions have only a small difference in areas, leading to significant cancellations in the total integral. However, this difference in areas is a little larger than that at $R = 3.0 \text{ \AA}$, where $\mu_g(r)$ is found to be even more clearly linear in the relevant r range. A modest intensity enhancement at $R = 2.8 \text{ \AA}$ compared to $R = 3.0 \text{ \AA}$ is therefore anticipated, and borne out by the plot in Figure 2.

For moderate strength H-bonds ($R \sim 2.6 \text{ \AA}$, middle panel), μ_g is seen to be more non-linear. This is a consequence of the shape of the mixing angle $\theta(r)$ with r [compare equations (8) and (9)]; with decreasing R , it changes less abruptly along r between its diabatic limits of 0 and $\pi/2$. As a consequence, the charge transfer character changes more continuously as the proton moves from the donor to the acceptor. This is true for $\mu_g(r)$ as well. Returning to the wavefunction product, the $\phi_{1^+}\phi_{0^-}$ overlap function has more unequal positive and negative spread at $R = 2.6 \text{ \AA}$. This results in less cancellation

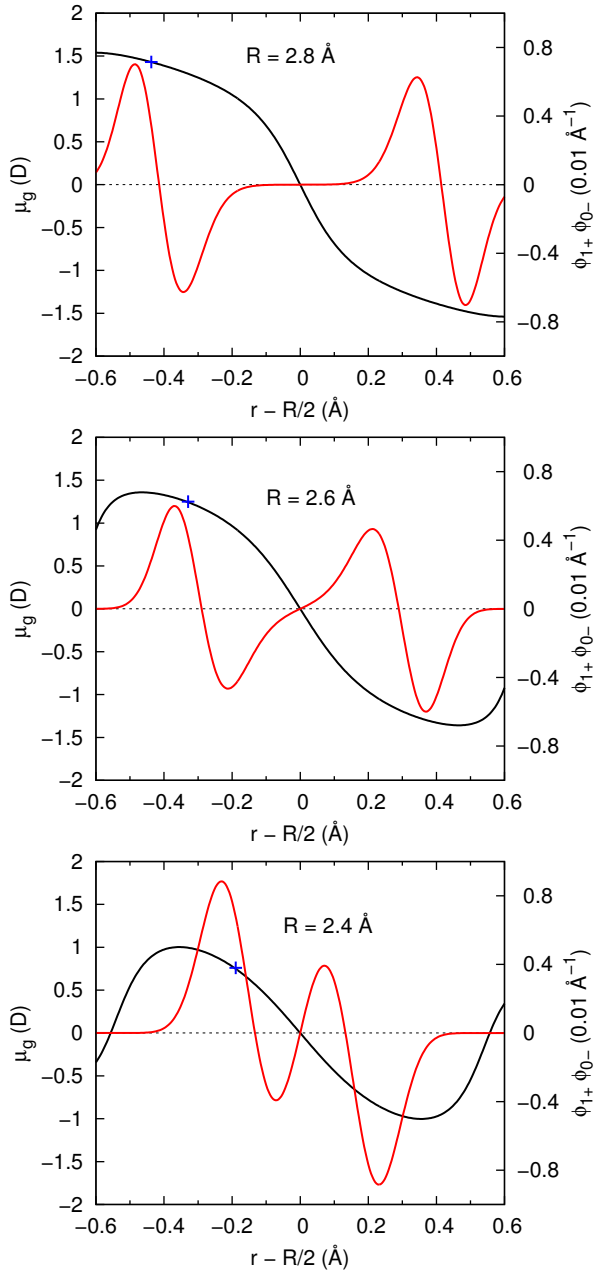


Figure 3: Origin of breakdown of the Condon approximation. Plotted are the dipole moment function $\mu_g(r)$ (black line, left axis) and the wavefunction overlap $\phi_{1+}\phi_{0-}$ (red line, right axis) as a function of $r - R/2$ for $R = 2.8, 2.6,$ and 2.4 Å. The product of these two functions is the integrand in the transition dipole matrix element (4). As the H-bond strength increases and R decreases, the wavefunction overlap has significant weight where the dipole function becomes non-linear. That is, as r gets closer to $R/2$, the slope of the dipole function is significantly larger than that at the equilibrium bond length. This non-linearity contributes to the enhanced absorption intensity. The blue plus sign marks the classical minimum of the (left-side of the) double-well for a given R . The dipole derivative in the Condon approximation, Eqn. (5), is evaluated at this point.

compared to the case at $R = 2.8$ Å, resulting in a larger enhancement of intensity. All these effects becomes stronger

still at $R = 2.4$ Å (bottom panel).

The dashed line in Figure 2 gives the intensity obtained using the Condon approximation (eqn.(4)). The required derivative of $\partial\mu_g/\partial r$ was evaluated at the classical minimum of the double well for each R . In Figure 3, these are marked with blue plus signs. In the weak H-bond region (large R), the intensity calculated through this approximation is in agreement with the actual value. But as R decreases the approximation breaks down and is seen to underestimate the intensity. Figure 3 helps explain this Condon breakdown. For weak H-bonds, $\mu_g(r)$ is largely linear in the region where $\phi_{1+}\phi_{0-}$ has significant amplitude, as seen for $R = 2.8$ Å. Taking a constant dipole derivative for this case is reasonable. But as the H-bond strengthens, $\mu_g(r)$ is sufficiently non-linear for $R = 2.6$ Å, and even more so at $R = 2.4$ Å. For these cases, the $\phi_{1+}\phi_{0-}$ overlap curve becomes less localized, i.e., broader. This reflects the large zero-point motion due to the reduced frequency of the OH stretch and the increase in anharmonicity and tunneling. Hence, the actual intensity is more enhanced than that calculated with the Condon approximation.

We now discuss in detail the results for asymmetric H-bonds. The trend for R in the range 2.7-3.0 Å is shown as the red curve in the inset of Figure 2. Here, too, there is an enhancement in intensity with decreasing R , albeit smaller than that for the symmetric case. At $R = 2.7$ Å, it is about 1.25 times that for a free OH. This fraction varies slightly when the asymmetry is changed to 40 or 75 kcal/mol, the former (latter) leading to higher (lower) intensity. Insight into why these numbers are all lower than the symmetric case may be obtained from the work of di Paolo et al.¹⁴ Translating their notation to ours, the fundamental intensity is proportional to $(\mu'_g - 5b\mu''_g)^2$, where the dipole derivatives are evaluated at the potential minimum, and b is the (dimensionless) ratio of the cubic anharmonicity to the harmonic frequency of the well. With $b < 0$ being the typical case, and μ'_g and μ''_g having the same sign (which is true in our case as well), di Paolo et al. argued that the second term augments the first. Therefore, the potential and electrical anharmonicity enhance the fundamental intensity. For our case, the symmetric case has both larger $|b|$ and larger μ''_g than the asymmetric one at a given R . The underlying cause is the larger mixing of diabats in the symmetric versus asymmetric models, ultimately leading to the computed differences in intensities.

C. Isotope effect on the intensity of the $1^+ \leftarrow 0^-$ transition

Experiments show that the intensity of the fundamental transition of a H-bonded O-H stretch mode is suppressed upon substituting H by D.⁵ The black curve of Figure 4 shows how H/D isotope substitution affects the intensity of the fundamental, as calculated for our symmetric H-bond model. (We limit the analysis to the symmetric case since the effects discussed below are more important in the medium and strong H-bonds.) The A_H/A_D ratio shows a non-monotonic dependence on R . In the weak H-bond region, the ratio is almost unaffected as R varies. Also, the Condon approximation holds well here: $A_H/A_D = 2$; see Section II. For H-bonds

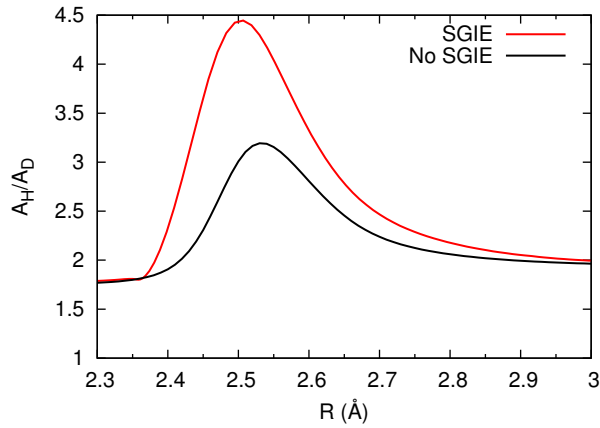


Figure 4: Isotope intensity ratio, A_H/A_D , for the $1^+ \leftarrow 0^-$ transition as a function of the donor-acceptor distance R . For the red (black) curve the secondary geometric isotopic effect (SGIE), i.e., change in the donor-acceptor distance R , is (is not) taken into account. The SGIE enhances the isotope intensity ratio for low-barrier H-bonds.

with moderate strength, the ratio increases reaching a maximum at $R \simeq 2.53$ Å. The position of this maximum roughly matches with the minimum of the frequency ratio in Figure 8 of Ref. 30. For still stronger H-bonds, the intensity ratio declines and becomes ~ 1.7 at very short R . This is attributed to the square-well-like behaviour of the potential for this range of R .³⁰ (For a square-well potential, the vibrational wavefunctions are independent of mass while the transition frequencies are mass dependent. Thus the ratio of intensities will mainly be due to the frequency ratio, which is approximately 2.)

Another important aspect of the isotope effect is the secondary geometric isotope effect (SGIE) where the O-O equilibrium distance is changed upon substituting H by D (Section II B). This modifies the adiabatic potential, which, in turn, also affects the intensity. Therefore, the experimental quantity that we need to calculate is $A_H(R_H)/A_D(R_D)$, where R_D is different from R_H due to SGIE. The red curve of Figure 4 shows this ratio. Evidently, this ratio is overall larger compared to the one without SGIE. The maximum is shifted to slightly lower R , and interestingly also roughly corresponds to the H/D frequency ratio minimum calculated with SGIE in Figure 8 of Ref. 31. Bratos et al.⁵ quotes the A_H/A_D ratio to be about 2, 2.6, and 3-5 for weak, moderate, and strong bonds, respectively. These are in agreement with our results that include the SGIE.

Insight into the observed trend of the A_H/A_D ratio with R can be given by analysing how the integrand of the transition dipole moment, $\phi_{1+\mu_g}(r)\phi_{0-}$, varies with r for each isotope at different R values. This product function is plotted in Figure 5 for O-O distances in the weak ($R = 2.8$ Å) and fairly strong ($R = 2.5$ Å) H-bond regions. The H (black) and D (blue) curves are without the inclusion of the SGIE. They are different essentially because H experiences larger anharmonicity effects than D. The wavefunctions for H have a greater spread than those for D. With $\mu_g(r)$ being the same for both, the product function plotted for H in both panels of

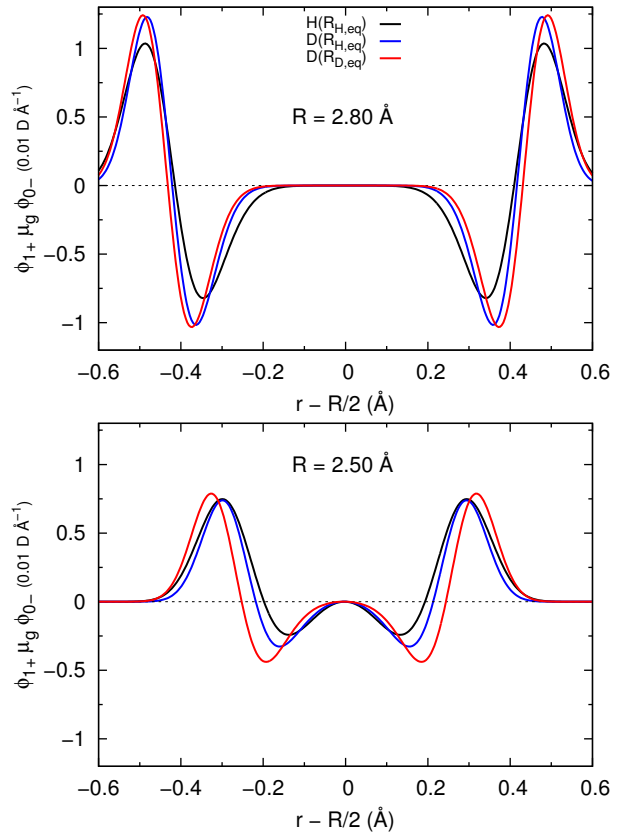


Figure 5: Integrand for the transition matrix element $\phi_{1+\mu_g}\phi_{0-}$ for the H and D isotopes for different R . The black curve is for H isotope while red and blue curves are for D isotope with and without the secondary geometric isotope effect (SGIE), respectively. The H-bond is stronger at lower R .

Figure 5 have larger positive than negative areas compared to those for D. Therefore, the transition dipole integral is higher for H than D. On including the SGIE μ_{1+0^-} (red curves), one sees very little change for weak bonding; the integrands with and without this effect are rather similar. For strong H-bonds, there is a clear difference. The resulting integrals for D are smaller and so A_H/A_D is higher.

D. Overtone intensity

Figure 6 shows the intensity of the $2^+ \leftarrow 0^-$ transition as a function of R for a symmetric H-bond. Its intensity for a monomeric OH (at $R = 6.0$ Å for our model) is about 0.32 km/mol. It has a complicated non-monotonic dependence on R . The inset shows that with decreasing R the intensity initially drops to zero at about 2.96 Å, and thereafter rises rapidly. This initial overtone suppression occurs at a distance somewhat larger than anticipated based on prior works, which indicate suppression up to at least 2.8 Å. We shall see further below that this might be a consequence of asymmetric H-bonds studied in those works. Continuing to smaller R or stronger H-bonds, we find the transition intensity going up to

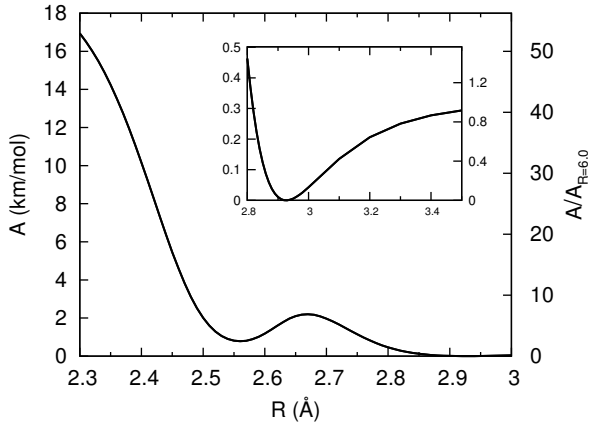


Figure 6: Dependence of the intensity of the $2^+ \leftarrow 0^-$ transition on R . The left axis is the intensity in units of km/mol and the right axis is the intensity scaled by its value for $R = 6.0 \text{ \AA}$ (absence of H-bond). This clearly shows the non-monotonic dependence of the overtone intensity on the strength of the H-bond. Furthermore, for medium to strong bonds, significant enhancement of the overtone intensity is possible. The inset shows the trend in the weak H-bonding region. Note that there is some intensity suppression near and above 3.0 \AA .

$\sim 17 \text{ km/mol}$, which is about a 50-fold enhancement. That the overtone is not suppressed at all distances, but instead increases to significant values compared to that for a free OH oscillator, is a new finding in this work.

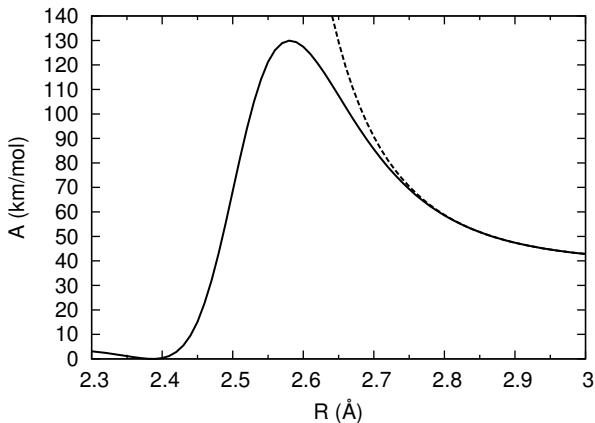


Figure 7: Dependence of the intensity of the $1^- \leftarrow 0^+$ transition on R . For this transition, the intensity for weak H-bonds ($R \sim 2.7$ to 3.0 \AA) is the same as that of the fundamental ($1^+ \leftarrow 0^-$) (shown as the dashed curve) since the tunnel-split ground and excited states are hardly distinct (compare Figure 1). It is only for stronger H-bonds that this transition may be considered distinct from the fundamental.

As argued in Section III A, the $1^- \leftarrow 0^+$ transition may also be labelled as the overtone for strong H-bonds. For example, at 2.45 \AA , it is this transition that is about twice the fundamental, while the $2^+ \leftarrow 0^-$ transitions has thrice the frequency. Figure 7 gives the variation for the intensity of this transition with R . It is of significance only when $R \lesssim 2.6 \text{ \AA}$, when it becomes distinct from the fundamental, due to observable tunnel splitting. When this happens the intensity has

a highly non-monotonic variation with R , quite distinct from the monotonic increase with bond strength of the $2^+ \leftarrow 0^-$ transition. In this region ($R \leq 2.6 \text{ \AA}$), the $1^- \leftarrow 0^+$ transition has a generally larger, but rapidly dropping, intensity compared to the $2^+ \leftarrow 0^-$ transition; note the ordinate scale of the two plots. Thus observing both frequency (Figure 1) range and intensity (Figures 6 and 7) variation will help distinguish the two overtones.

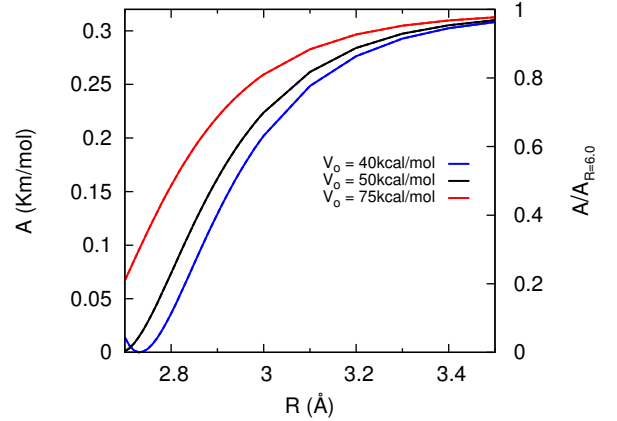


Figure 8: Intensity of the $2^+ \leftarrow 0^-$ overtone transition for different asymmetries, viz. $V_o = 40, 50,$ and 75 kcal/mol . These plots contrast to the symmetric case (inset of Figure 6), showing that the extent and donor-acceptor distance range of overtone suppression in an H-bond (relative to a free OH) changes when the double-well potential is asymmetric. The plots also show that these properties can vary with the amount of asymmetry (V_o).

We now return to the weak H-bonding region, and discuss the effect of asymmetry on the double well potential. Plots of the $2 \leftarrow 0$ transition using $V_o = 40, 50,$ and 75 kcal/mol are shown in Figure 8. Note that the applied V_o are all sizeable compared to the OH dissociation energy (Morse parameter D here is 120 kcal/mol). Although the shifted right diabats lie higher than the Morse overtone level (about 25 kcal/mol above the potential minimum) for all cases, the overtone intensity trends are different for each V_o . Importantly, though, all of them lower the O-O distance range for overtone suppression to at least 2.8 \AA . It is difficult to ascertain the precise cause of this change, but our calculations show that overtone properties are rather sensitive to the shape of the anharmonic potential and the resulting μ_g as well. Indeed, it is this sensitivity that leads to the curious trend in Figure 6.

However, a qualitative understanding of the trends between the three V_o values of Figure 8 may be obtained through the work of di Paolo et al.¹⁴. They give the overtone intensity to be proportional to $(\mu'_g b + \mu''_g)^2$. (See the end of Section III B for the notation.) As such, with $b < 0$ and the derivatives have the same sign, the two parts of the sum compete with each other. (This leads to a qualitative explanation for overtone suppression.) As V_o increases, we may expect the anharmonicity parameter b to decrease (towards its Morse value). Assuming that the dipole derivatives are approximately constant over the chosen V_o range, the overtone intensity would increase with V_o at a given R . The plots also show the over-

tone is less suppressed at higher V_o .

E. Effect of variation of the dipole function

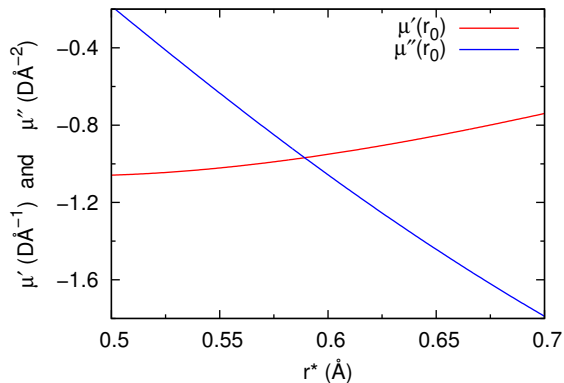


Figure 9: Parameter sensitivity of the dipole derivatives. First and second derivatives of the Mecke function, $\mu_0(r) = \mu^* r \exp(-r/r^*)$, evaluated at $r = r_0 = 0.96 \text{ \AA}$ for a range of r^* values. The OH bond r^* value of 0.6 \AA , given by Lawton and Child³⁹, has been used in all earlier plots in this work. The first and second derivatives are relevant to the intensity of the fundamental and overtone transitions, respectively. Note that the first derivative varies little for the parameter range shown whereas the second derivative varies by a factor of about five.

The shape of $\mu_g(r)$ [Eq. (12)] is dependent on that of the diabatic dipole function, $\mu_0(r)$. We have used the two-parameter Mecke function form for $\mu_0(r)$ in this work. As Eq. (14) shows, the parameter r^* governs its shape while μ^* gives it magnitude. We now analyse how the fundamental and overtone intensities change when r^* is varied around its Lawton-Child value of 0.6 \AA for the OH bond. The results below are for symmetric H-bonds.

The value of r^* marks the position of the Mecke function maximum. When varied, it is useful to know how the first and second derivatives of μ_0 change at the reference OH distance of $r = r_0 = 0.96 \text{ \AA}$. Figure 9 shows that the first derivative $\mu'_0(r_0)$ changes within about 20% as r^* is varied from 0.5 to 0.7 \AA . However, the second derivative $\mu''_0(r_0)$ changes more substantially, doubling at 0.7 \AA and reducing at 0.5 \AA to 20% of the original value (at $r^* = 0.6 \text{ \AA}$). This suggests that changing r^* , and hence μ_g , might result in a noticeable but fractional change on the fundamental intensity, but substantially alter the intensity of the overtone.

Figure 10 shows the $1^+ \leftarrow 0^-$ fundamental (top panel) and $2^+ \leftarrow 0^-$ overtone (bottom panel) intensities as a function of R for different r^* values. For the fundamental, the intensity changes with r^* appear larger for strong H-bonds (lower R). However, these are only a consequence of the uniform scale of the plot's y -axis. The intensities for successive r^* values generally differ by about 10-20% at both large and small R . In effect, variation in the fundamental intensities with the shape parameter of the diabatic dipole function is modest. We note that for $R \gtrsim 2.8 \text{ \AA}$, the intensity is lower for larger r^* , con-

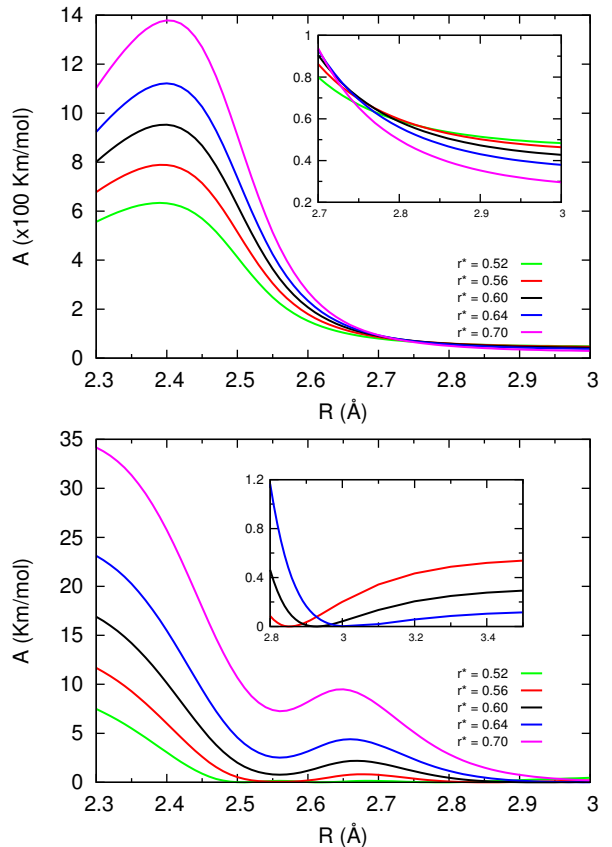


Figure 10: Variation of fundamental (top panel) and overtone (bottom panel) intensity with R for different Mecke parameters r^* . The $r^* = 0.6 \text{ \AA}$ curves are both the same as those in Figures 2 and 6. The top panel shows that the fundamental enhancement is only somewhat affected by r^* , especially for weak bonds, while the overtone intensities change more dramatically. The fundamental intensities show a curious trend switch around 2.75 \AA , which is shown in the inset and analysed in the main text.

tent with the Mecke function derivatives discussed above. But this trend is reversed for $R \lesssim 2.75 \text{ \AA}$: The intensity enhancement is larger (smaller) for larger (smaller) r^* . We briefly analyse this trend.

All components of the transition moment integral $\langle \phi_{1+} | \mu_g | \phi_{0-} \rangle$ vary with R , but only $\mu_g(r)$ changes with r^* . We rewrite the integral as $\mu_{g,n} \langle \phi_{1+} | \mu_g / \mu_{g,n} | \phi_{0-} \rangle = \mu_{g,n} \langle S \rangle$. We take $\mu_{g,n} \equiv \mu_g(r = r_{node})$, where r_{node} is the (non-central) node of the wavefunction product (shown in Figure 3) for that R . Note that r_{node} does not shift with r^* at a given R , and therefore provides a common reference point at that R . In this manner, the transition moment is separated into a shape part, $\langle S \rangle$ and an overall magnitude, $\mu_{g,n}$. Though not shown, we found that plots of $\mu_g / \mu_{g,n}$ for various R and r^* look nearly the same. Table I shows the intensity contributions of these pieces for $r^* = 0.56$ and 0.64 \AA , relative to those at $r^* = 0.6 \text{ \AA}$. For the shorter distances ($R = 2.6$ and 2.4 \AA), the relative intensities (A ratios) are about the same as the relative $\mu_{g,n}^2$. The ratio of $|\langle S \rangle|^2$ is nearly unity, so the shape of the dipole function plays a minor role. However, for

Table I: Contribution to the fundamental intensity at different value of Mecke parameter r^* . Compared are the total intensity (A), the scale factor ($\mu_{g,n}$) and the matrix element of $\mu_g/\mu_{g,n}$, denoted $\langle S \rangle$. All results are reported as ratios relative to the results for $r^* = 0.6$; the $^\circ$ superscript in the table header indicates the value of the quantity for $r^* = 0.6$. The final column is obtained as a ratio of the middle two.

R (Å)	A/A°	$ \mu_{g,n}/\mu_{g,n}^\circ ^2$	$ \langle S \rangle/\langle S \rangle^\circ ^2$
$r^* = 0.56$			
2.8	1.02	0.89	1.15
2.6	0.87	0.89	0.97
2.4	0.83	0.80	1.03
$r^* = 0.64$			
2.8	0.95	1.11	0.86
2.6	1.13	1.10	1.02
2.4	1.12	1.18	0.94

weak H-bonds, the shape appears to play a role. At $R = 2.8$ Å, it overrides the effect of $\mu_{g,n}$.

For the overtone, the bottom panel of Figure 10 shows that although overall shape remains about the same, the intensity drops strongly with decreasing r^* . This appears in agreement with the variation in $\mu_0''(r_0)$ discussed at the start of this section. However, for weak H-bonds, shown in the inset is a trend reversal. Indeed, in this region the μ_0'' -based analysis is expected to be more valid. This suggests that overtone intensities in this context are perhaps not easily analysed by way of derivatives, and that details of the transition moment integrand, viz. $\psi_{2^+}\mu_g\psi_{0^-}$, do matter. Another aspect that the inset points to is that the extent and range of overtone suppression in the weak H-bonding range is a sensitive function of r^* .

IV. COMPARISON WITH PREVIOUS WORK

We have already noted in earlier sections that that our results for the fundamental enhancement in Figure 2 (solid line) and the corresponding A_H/A_D ratio in Figure 4 with SGIE are in overall agreement with experimental ranges summarised by Bratos et al.⁵; see Sections III B and III C. We now consider some specific molecular systems.

A. Symmetric H-bonds

Bournay and Marechal⁴² measured the isotope intensity ratio for acetic acid dimers in the gas phase (which have $R \simeq 2.68$ Å⁴³), finding a ratio of 2 ± 0.2 for the transition probabilities (i.e., $|\mu_{fi}|^2$). Owing to a marked departure from the harmonic value $\sqrt{2}$, they suggested the value to be anomalous, and attributed it to a breakdown of the Born-Oppenheimer approximation. However, our model is within this approxima-

tion. At that O-O distance, Fig. 4 gives $A_H/A_D \simeq 2.6$, while the frequency ratio $\nu_H/\nu_D \simeq 1.3$ from Figure 8 of Ref. 30. This yields a transition probability of about 2.0, which agrees with their measurements. In contrast, our estimate of about 5 for the H isotope's $|\mu_{fi}|^2$ enhancement compared to the monomer is much lower than their experimental estimate of about 32.

A number of theoretical and experimental studies have been performed on the Zundel cation, H_5O_2^+ , which has $R \simeq 2.5$ Å. More recently, Tan and Kuo⁴⁴ studied $(\text{CH}_3\text{OH})_2\text{H}^+$, which has $R \simeq 2.4$ Å. For the Zundel cation, one of the peaks around 1000 cm^{-1} is identified with the proton transfer motion, which would correspond to the $0^- \leftarrow 0^+$ transition in the notation of present work; see our footnote in Ref. 45. Unfortunately, an experimental measurement of the absolute intensity seems unavailable. Theoretical studies also give the relative intensities of this mode to be 3-10,⁴⁶ 8,⁴⁷ and 20-40⁴⁸ times the intensity of the OH stretches of the end groups. For $(\text{CH}_3\text{OH})_2\text{H}^+$, the OH stretch at 1010 cm^{-1} (also $0^- \leftarrow 0^+$ in our notation) was computed to have an intensity of 2567 km/mol⁴⁴.

In the present work for $R = 2.5$ Å and 2.4 Å, the $0^- \leftarrow 0^+$ transition has frequencies of about 164 and 750 cm^{-1} , respectively. Clearly, these are lower than those of the aforementioned works. The corresponding intensities are about 335 and 600 km/mol, or enhancements of about 9 and 15. (Note that these are relative to $1^+ \leftarrow 0^-$ at $R = 6.0$ Å.) At the same R values, $1^+ \leftarrow 0^-$ frequencies are 1620 and 1780 cm^{-1} , which err on the higher side compared to the Zundel and $(\text{CH}_3\text{OH})_2\text{H}^+$ cations. The corresponding intensities are about 625 and 950 km/mol, i.e. 16 and 24-fold enhancement.

We end this section with a brief comparison with a particle in a box (PIB) model. For short, strong H-bonds the potential appears similar to that for a PIB of width $L = R - 2r_0$ with quantum numbers $n = 1, 2, 3, \dots$ ³⁰. The corresponding transition dipole moment for a transition $n_f \leftarrow n_i$, is only non-zero when $n_f - n_i$ is odd, for which $A_{if} \propto (n_f^2 n_i^2)/(n_f^2 - n_i^2)^3$ is box-length independent. Here, the three transitions $3 \leftarrow 2$, $4 \leftarrow 1$, and $5 \leftarrow 2$, in the PIB. correspond to $1^+ \leftarrow 0^-$, $1^- \leftarrow 0^+$, and $2^+ \leftarrow 0^-$, respectively, in the strong H-bond case. In the PIB, the three transitions have the intensity ratios about 60:1:2. Figures 2, 6 and 7 suggest that the ratios are roughly comparable, but are still clearly R -dependent unlike the PIB case.

B. Asymmetric H-bonds

The molecular system discussed below are weak H-bonds. For numerical comparisons, we will use our asymmetric model with $V_o = 50 \text{ kcal/mol}$. Note, however, that this choice of V_o is not special. Our results do vary somewhat with V_o , as Figure 8 demonstrates. For the fundamentals alone, we additionally quote our symmetric model results for contrast. Also, if the H-bonded O-O distance was not directly available from the cited work, it was estimated using the given OH fundamental red-shift and Figure 1.

For the fundamental of ethanol dimers, Provencal et al.²²

calculated an enhancement of 10-20 relative to the monomer in the double harmonic approximation. For intramolecularly H-bonded propane- and butanediol, Howard and Kjaergaard⁹ report the OH stretch intensity to be enhanced 4-11 times for different conformers. These H-bonds have $R \simeq 2.8 - 2.9 \text{ \AA}$, for which our enhancement factors are 1.3-1.5 for the symmetric model and 1.07-1.12 for the asymmetric model. Suhm and co-workers¹⁰ experiments on 2,2,2-trifluoroethanol dimers show an intensity enhancement of 4.0 ± 0.8 for the fundamental of the donor O-H compared to the acceptor O-H. Our values are about 1.26 and 1.04 for the symmetric and asymmetric cases. In general, the enhancement from our calculation for $R \gtrsim 2.7 \text{ \AA}$ is at most ~ 2 with the symmetric model and ~ 1.2 with the asymmetric model (see inset of Figure 2), both of which are smaller than values in the literature.

For the same molecules, however, our overtone suppression estimate compares somewhat more favourably. Suhm and coworkers reported a value of A/A_{free} for 2,2,2-trifluoroethanol dimer to be 0.3 ± 0.1 ¹⁰. Our estimate is 0.63. Calculations by Howard and Kjaergaard⁹ for propane- and butanediols indicate a suppression from 0.43 to 0.15, with lower values for butanediols. Our estimates are consistent with this relative ordering of magnitudes and in the range 0.41 to 0.20. In general, literature values of A/A_{free} for the overtone are about 0.5 to 0.1, the smaller values pointing to stonger H-bonds. Figure 8 indicates (for R between 2.8 and 3.0 \AA) that our estimates are in about that range, allowing for variation of the asymmetry parameter V_o .

Finally, we discuss another metric, namely the fundamental-to-overtone intensity ratio, A_1/A_2 . This ratio is typically about 10 for monomers, and is reported to increase by over an order of magnitude with H-bonding^{10,11,21} in the weak region. For 2,2,2-trifluoroethanol dimer, Scherge et al.¹⁰ report $A_1/A_2 = 400 \pm 100$ and 30 ± 10 for the donor and acceptor O-H bonds, respectively. Our A_1/A_2 ratios are about 366 and 218, respectively. The experimental monomer ratio of 13 ± 2 is smaller than our ($R = 6.0 \text{ \AA}$) estimate of about 122. A more recent work from the Suhm group on the dimers of methanol, ethanol and t-butyl alcohol¹¹ gives the A_1/A_2 ratio for the donor O-H as 320 ± 90 , 400 ± 100 and 1000 ± 400 . Using values of R deduced from redshifts, our ratios are ≈ 493 , 583, and 711, in reasonable accord with experiment.

We also mention that some O-H \cdots Y-type asymmetric complexes have been analysed, e.g. $\text{F}^- \cdot \text{H}_2\text{O}$ ⁴⁹ and $\text{Cl}^- \cdot \text{H}_2\text{O}$ ⁵⁰ in theoretical studies. The former has a strong H-bond, for which an OH fundamental intensity enhancement of about 35 was computed (in the double harmonic approximation). For the chloride complex, it was found to be 50 using an anharmonic treatment. It also showed overtone suppression of 0.35. We have not attempted any numerical comparisons for these cases, since our model is parametrized for O-H \cdots O systems.

V. SUMMARY AND CONCLUDING REMARKS

We have discussed the intensity variation of the fundamental and overtone transitions in O-H \cdots O type H-bonds. The results are based on a diabatic two-state potential model and a Mecke form for the diabatic dipole moment. These yield a ground adiabat and associated adiabatic dipole moment along the H-atom transfer coordinate. The latter along with one-dimensional vibrational wavefunctions were used to compute the intensities for a range of O-O distances. Over this range, the H-bond varies from weak to strong. Also analysed are the role of donor-acceptor asymmetry (i.e. difference in their pK_a 's) as well as the effect of the shape of the Mecke function for the dipole moment.

For the OH fundamental, we find that the intensity is enhanced compared to the free OH over all relevant O-O distances, ranging from a factor of under 2 for weak H-bonds to about 20 for strong bonds. We show that the non-linearity of the dipole moment is important, especially for medium and strong H-bonds, and therefore the Condon approximation is not suitable. The H/D isotope effect was analysed in terms of the fundamental intensity ratio, which is found to be non-monotonic with H-bond strength. A maximum occurs for this ratio at the donor-acceptor distance R of about 2.5 \AA , and the secondary geometric isotope effect plays an important role in the height and position of this maximum. For the OH overtone, our model finds intensity suppression for weak H-bonds, and shows variability in magnitude and R_{OO} range depending on whether we consider symmetric or asymmetric bonds. For medium and strong H-bonds, enhancements in the intensity are seen with the symmetric model, going up to 50 times the free OH value. This new finding suggests that overtones should be easily experimentally visible for such H-bonds.

Our results are generally consistent in trends but differ in numbers with previous work, including both experimental and theoretical studies. In particular, our enhancements in fundamental intensities for weak H-bonds are clearly lower. Comparisons of overtone suppression in the same region with the asymmetric model fare somewhat better. These comparisons suggest that in regime of weak asymmetric bonds that our simple model may be missing some key physical ingredient. Variations in shape of the dipole moment function lead to modest fractional change in the intensity of the fundamental, but to larger changes for the overtone.

Studies of H-bond intensities offer an excellent point of comparison for experiment and theory, owing to the large spread of bonding strengths and topologies. In the present context of O-H \cdots O H-bonds, with a few exceptions such as H_5O_2^+ and $(\text{CH}_3\text{OH})_2\text{H}^+$, most detailed studies have mainly focussed on specific systems in the weak H-bonding regime. Experiments on symmetric medium and strong H-bonded systems are desirable. Some possible candidates are carboxylic acid dimers ($R \simeq 2.45 \text{ \AA}$), HCrO_2 ($R \simeq 2.49 \text{ \AA}$), porphycenes⁵¹, and proton sponges⁵², for which the fundamental, first overtone, and isotope effect could be measured and analysed. Slightly asymmetric biomolecular systems with strong H-bonds that could be investigated include mutated GFP⁵³, photoactive yellow protein⁵⁴ and the enzyme KSI⁵⁵.

Acknowledgments

We thank Seth Olsen for helpful discussions.

-
- * Electronic address: email: r.mckenzie@uq.edu.au; URL: URL: condensedconcepts.blogspot.com
- ¹ E. Arunan, G. R. Desiraju, R. A. Klein, J. Sadlej, S. Scheiner, I. Alkorta, D. C. Clary, R. H. Crabtree, J. J. Dannenberg, P. Hobza, et al., *Pure and Applied Chemistry* **83**, 1619 (2011).
 - ² C. Pimentel, George and L. McClellan, Aubrey, *The Hydrogen Bond* (W. H. Freeman And Company, 1960).
 - ³ Y. Marechal and A. Witkowski, *J. Chem. Phys.* **48**, 3697 (1968).
 - ⁴ S. Bratos, *J. Chem. Phys.* **63**, 3499 (1975).
 - ⁵ S. Bratos, H. Ratajczak, and P. Viot, in *Hydrogen-Bonded Liquids* (Springer, 1991), pp. 221–235, [Note: The intensity ratio for isotopes in this reference appears to be the square of the dipole matrix element ratio alone. We use their values after multiplication with the frequency ratio they have given.]
 - ⁶ F. Fillaux, *Chemical Physics* **74**, 395 (1983).
 - ⁷ A. Iogansen, *Spectrochimica Acta Part A: Molecular and Biomolecular Spectroscopy* **55**, 1585 (1999).
 - ⁸ C. Burnham, G. Reiter, J. Mayers, T. Abdul-Redah, H. Reichert, and H. Dosch, *Physical Chemistry Chemical Physics* **8**, 3966 (2006).
 - ⁹ D. L. Howard and H. G. Kjaergaard, *The Journal of Physical Chemistry A* **110**, 10245 (2006).
 - ¹⁰ T. Scharge, D. Luckhaus, and M. A. Suhm, *Chemical Physics* **346**, 167 (2008).
 - ¹¹ F. Kollipost, K. Papendorf, Y.-F. Lee, Y.-P. Lee, and M. A. Suhm, *Phys. Chem. Chem. Phys.* **16**, 15948 (2014).
 - ¹² H. Ratajczak, W. Orville-Thomas, and C. Rao, *Chemical Physics* **17**, 197 (1976).
 - ¹³ M. Rozenberg, *RSC Adv.* **4**, 26928 (2014).
 - ¹⁴ T. D. Paolo, C. Bourdéron, and C. Sandorfy, *Canadian Journal of Chemistry* **50**, 3161 (1972).
 - ¹⁵ G. E. Hilbert, O. R. Wulf, S. B. Hendricks, and U. Liddel, *Journal of the American Chemical Society* **58**, 548 (1936).
 - ¹⁶ E. Heller, *The Journal of Physical Chemistry A* **103**, 10433 (1999).
 - ¹⁷ K. K. Lehmann and A. M. Smith, *J. Chem. Phys.* **93**, 6140 (1990).
 - ¹⁸ E. S. Medvedev, *J. Chem. Phys.* **137**, 174307 (2012).
 - ¹⁹ P. F. Bernath, *Spectra of Atoms and Molecules* (Oxford University Press, 2005), 2nd ed.
 - ²⁰ W. Zou and D. Cremer, *Theor Chem Acc* **133** (2014).
 - ²¹ J. Phillips, J. Orlando, G. Tyndall, and V. Vaida, *Chemical Physics Letters* **296**, 377 (1998).
 - ²² R. A. Provencal, R. N. Casaes, K. Roth, J. B. Paul, C. N. Chapo, R. J. Saykally, G. S. Tschumper, and H. F. Schaefer, *J. Phys. Chem. A* **104**, 1423 (2000).
 - ²³ K. Kuyanov-Prozument, M. Y. Choi, and A. F. Vilesov, *The Journal of Chemical Physics* **132**, 014304 (2010).
 - ²⁴ E. U. Condon, *Physical Review* **32**, 858 (1928).
 - ²⁵ S. Wang, *Phys. Rev. A* **60**, 262 (1999).
 - ²⁶ J. Vazquez and J. F. Stanton, *Molecular Physics* **104**, 377 (2006).
 - ²⁷ S. Banik and M. Durga Prasad, *Theor. Chem. Acc.* **131**, 1282 (2012).
 - ²⁸ J. Schmidt, S. Corcelli, and J. Skinner, *J. Chem. Phys.* **123**, 044513 (2005).
 - ²⁹ R. H. McKenzie, *Chemical Physics Letters* **535**, 196 (2012).
 - ³⁰ R. H. McKenzie, C. Bekker, B. Athokpam, and S. G. Ramesh, *The Journal of Chemical Physics* **140**, 174508 (2014).
 - ³¹ R. H. McKenzie, B. Athokpam, and S. G. Ramesh, *The Journal of Chemical Physics* **143**, 044309 (2015).
 - ³² G. Gilli and P. Gilli, *The Nature of the Hydrogen Bond* (Oxford U.P., Oxford, 2009).
 - ³³ W. H. Thompson and J. T. Hynes, *Journal of the American Chemical Society* **122**, 6278 (2000).
 - ³⁴ J. M. Robertson and A. R. Ubbelohde, *Proceedings of the Royal Society A: Mathematical, Physical and Engineering Sciences* **170**, 222 (1939).
 - ³⁵ M. Ichikawa, *Journal of Molecular Structure* **552**, 63 (2000).
 - ³⁶ N. Sokolov, M. Vener, and V. Savel'ev, *Journal of Molecular Structure* **177**, 93 (1988).
 - ³⁷ A. Nitzan, *Chemical Dynamics in Condensed Phases: Relaxation, Transfer and Reactions in Condensed Molecular Systems* (Oxford University Press, 2006).
 - ³⁸ R. Mecke, *Zeitschrift für Elektrochemie und angewandte physikalische Chemie* **54**, 38 (1950).
 - ³⁹ R. T. Lawton and M. S. Child, *Molecular Physics* **40**, 773 (1980).
 - ⁴⁰ W. Jakubetz, J. Manz, and V. Mohan, *The Journal of Chemical Physics* **90**, 3686 (1989).
 - ⁴¹ F. Grossmann, *Theoretical Femtosecond Physics: Atoms and Molecules in Strong Laser Fields* (Springer Science & Business Media, 2013).
 - ⁴² J. Bournay and Y. Marechal, *J. Chem. Phys.* **59**, 5077 (1973).
 - ⁴³ J. L. Derissen, *Journal of Molecular Structure* **7**, 67 (1971).
 - ⁴⁴ J. A. Tan and J.-L. Kuo, *Journal of Physical Chemistry A* **119**, 11320 (2015).
 - ⁴⁵ There is debate about the correct identification of features in the IR spectra, due to large anharmonic and intermode coupling effects, requiring a high-dimensional potential energy surface.
 - ⁴⁶ M. V. Vener, O. Kühn, and J. Sauer, *The Journal of Chemical Physics* **114**, 240 (2001).
 - ⁴⁷ O. Vendrell, F. Gatti, and H.-D. Meyer, *The Journal of chemical physics* **127**, 184303 (2007).
 - ⁴⁸ T. L. Guasco, M. A. Johnson, and A. B. McCoy, *The Journal of Physical Chemistry A* **115**, 5847 (2011).
 - ⁴⁹ B. F. Yates, H. F. Schaefer, T. J. Lee, and J. E. Rice, *Journal of the American Chemical Society* **110**, 6327 (1988).
 - ⁵⁰ A. B. McCoy, *The Journal of Physical Chemistry B* **118**, 8286 (2014).
 - ⁵¹ P. Cika, P. Fita, A. Listkowski, M. Kijak, S. Nonell, D. Kuzuhara, H. Yamada, C. Radzewicz, and J. Waluk, *The Journal of Physical Chemistry B* **119**, 2292 (2015).
 - ⁵² Y. Horbatenko and S. F. Vyboishchikov, *ChemPhysChem* **12**, 1118 (2011).
 - ⁵³ L. M. Oltrogge and S. G. Boxer, *ACS Central Science* **1**, 148 (2015).
 - ⁵⁴ M. Nadal-Ferret, R. Gelabert, M. Moreno, and J. M. Lluch, *Journal of the American Chemical Society* **136**, 3542 (2014).
 - ⁵⁵ L. Wang, S. D. Fried, S. G. Boxer, and T. E. Markland, *Proceedings of the National Academy of Sciences* **111**, 18454 (2014).